
Universiteit
Leiden
The Netherlands

Convergent molecular evolution of toxins in the venom of advanced snakes (Colubroidea)

Xie, B.

Citation
Xie, B. (2022, March 1). *Convergent molecular evolution of toxins in the venom of advanced snakes (Colubroidea)*. Retrieved from https://hdl.handle.net/1887/3277031

Version:	Publisher's Version
License:	Licence agreement concerning inclusion of doctoral thesis in the Institutional Repository of the University of Leiden
Downloaded from:	https://hdl.handle.net/1887/3277031

Note: To cite this publication please use the final published version (if applicable).

Chapter 3. Evolutionary Novelties in the Kunitz-type Toxins

This chapter is published as part of:

Bing Xie, Daniel Dashevsky, Darin Rokyta, Parviz Ghezellou, Behzad Fathinia, Qiong Shi, Michael K. Richardson and Bryan G. Fry. Dynamic genetic differentiation drives the widespread structural and functional convergent evolution of snake venom proteinaceous toxins. *BMC Biology*, 2022, 20:4. https://doi.org/10.1186/s12915-021-01208-9

Abstract

Kunitz-type toxins from snake venoms have undergone extraordinary structural and functional molecular adaptation. These toxins may have functions ranging from enzyme inhibitors to channel-blocking neurotoxins. However, their detailed evolutionary history is not known. We therefore conducted a large-scale phylogenetic and selection analysis to illustrate this issue. Phylogenetic analysis and analysis of selection revealed that the kunitz-type toxins evolved by gene duplication and rapid diversification. We show that the main ancestral function of kunitz-type toxins in Viperidae (plasmin inhibitors) is under neutral selection, while in non-vipers it is under purifying selection. We also show that neurotoxic kunitz-type toxins are found only in non-vipers; the various neurotoxic types clustered in distinct clades under positive selection. These results provide a detailed roadmap for future work to elucidate predator-prey evolutionary arms races, as well as documenting rich biodiscovery resources for lead compounds in the drug design and discovery pipeline.

Keywords: Kunitz, protease inhibitor, neurotoxin, evolution

Introduction

Toxins of the Kunitz type are interesting. According to their functions, they may be divided into two groups. Then there are the inhibitors of serine proteases and neurotoxins that block channels, such as dendrotoxins (DTX) and the B chain of bungarotoxin, constituting the second kind (BTX-b). The neurotoxins have a kunitz-like domain, although their protease inhibitory action is minimal. They are an example of dual convergence: not only have they been separately recruited into the venom arsenal of different species, but they are also convergently apotypic in multiple lineages for the same neurotoxic and coagulopathic properties (Beress 1982; Antuch, et al. 1993; Minagawa, et al. 1997; Harvey and Robertson 2004; Bayrhuber, et al. 2005; Honma and Shiomi 2006; Fry, Scheib, van der Weerd, Young, McNaughtan, Ramjan, Vidal, Poelmann and Norman 2008; Koludarov, et al. 2012).

Kunitz-type protease inhibitors attach to the active site of serine proteases predominantly through an exposed binding loop in a canonical configuration. P3, P2, P1, P1, P1, P2, and P3 (nomenclature according to Schechter and Berger) are the six residues that potentially interact with the enzyme in this area. A catalytic trio of residues on the enzyme's pocket (typically Ser, His, and Asp) is responsible for amide bond hydrolysis. In textilinin-1, this hexapeptide is Pro-Cys-Arg-Val-Arg-Phe (PCRVRF) (Flight, et al. 2009), whereas in aprotinin it is Pro-Cys-Lys-Ala-Arg-lle (PCKARI) (Wells and Strickland 1994). The P1 residue, whose side chain protrudes into the specificity pocket of the protease, is Arg in textilinin-1 and Lys in aprotinin.

Despite the large size of the kunitz-type protease inhibitors, they can be divided into three categories based on their target: trypsin inhibitors (positively charged residues Lys/Arg preferred at P1), elastase inhibitors (small hydrophobic residues Ala/Val at P1), and chymotrypsin inhibitors (large hydrophobic residues Phe/Trp/Tyr/Leu/Val at P1) (Laskowski Jr and Kato 1980; Hedstrom 2002; Wang, et al. 2012). Met, Asn and His at the P1 site residues were also reported for chymotrypsin inhibiting (Laskowski Jr and Kato 1980; Scheidig, et al. 1997; Chang, et al. 2001; Chen, et al. 2001; Guo, et al. 2013). The interaction inhibitor: trypsin is essentially independent of the nature of the basic residue at P1 position, with no substantial changes in the association energies with trypsin following the mutation K15R in BPTI, according to analysis of different mutants of BPTI and other trypsin inhibitors (Navaneetham, et al. 2010). Inhibition of kallikrein prefers Arg over Lys (Fieldler 1987; Grzesiak, et al. 2000), but plasmin inhibition is increased by Lys at the P1 site (Van Nostrand, et al. 1995). A hydrophobic amino acid residue (Ala, Gly, or Phe) binds to the P1′ site of venom trypsin/chymotrypsin inhibitors, with Ala being the most prevalent. AvKTI (Araneus ventricosus Kunitz-type serine protease inhibitor), which has the basic amino acid Lys (K) within the P1 site, has dual antitrypsin and antichymotrypsin action (Wan, et al. 2013). A snake venom serine protease inhibitor with Lys (K) at the P1 site and dual inhibitory action against trypsin and chymotrypsin was shown to have a similar effect (Guo, et al. 2013). Furthermore, the P1-P1 residues in AvKTI are Lys (K) and Ala (A), as shown for bovine pancreatic trypsin inhibitor (BPTI), which not only inhibits trypsin but also chymotrypsin, plasmin, and kallikrein. Kunitz peptides that inhibit plasmin are invariably dual-functional, with a P1 site of Arg (R) inhibiting both trypsin and plasmin. P1 and P1 are important residues. P1 fits into the pocket of human plasmin and interacts with six plasmin residues.

In this study, we applied the Bayesian method to reconstruct a large-scale phylogeny so as to reveal the evolution history of the snake venom kunitz-type toxins, particularly the evolutionary traits of the neurotoxic types. Analysis of selection was also utilized to evaluate the selection pressure on different toxin types.

Materials and Methods

Sequence Alignments and Phylogenetic Reconstruction

Protein sequences for all toxin sequences were retrieved from the UniProt database (https://www.uniprot.org) and NCBI database (http://www.ncbi.nlm.nih.gov), then combined with the toxin transcripts from our assembly and annotation (Chapter 2). Partial sequences, sequences with suspect assembling errors were excluded. For the blocks of sequence in between these sites, the sequences were aligned using a mix of manual alignment of the conserved cysteine locations and alignment using the Multiple Sequence Comparison by Log-Expectation (MUSCLE) method (Edgar 2004) implemented in AliView (Larsson 2014). Manual refinement of the alignment was also involved because there are structural differences within different toxin families. The phylogenetic trees for different toxin families were reconstructed with MrBayes 3.2 (Ronquist, et al. 2012) based on the amino acid sequence alignment. The settings for MrBayes can be found in the Supplementary File 2. The output trees from MrBayes were midpoint rooting, then further edited and annotated with iTol (Letunic and Bork 2007).

Tests for Selection

Coding DNA sequences, which are corresponding to the toxin sequences used for phylogenetic analysis, were retrieved from GenBank (Benson, et al. 2012) and our assembly. Using AliView and the MUSCLE method, the sequences were trimmed to only containing codons that translate to the mature protein, then translated, aligned, and reverse translated. Clades were created based on taxonomy and structural differences (functional domains/motifs, for example). The resultant codon alignments were used to create phylogenetic trees for each clade using the same methods outlined in the ‘Phylogenetic Reconstruction' section. All following studies were conducted using these tree topologies.

Calculating the ratio of nonsynonymous nucleotide substitutions per nonsynonymous site (dN) to synonymous substitutions per synonymous sites (dS) (ω=dN/dS) for each codon in the alignment might reveal if a gene is undergoing rapid evolution or stays functionally restricted. Codons developing with $\omega > 1$ are thought to have evolved under positive selection (functional diversity), whereas codons evolving with $\omega < 1$ are thought to have evolved under purifying selection. Sites with a value of $\omega = 1$ are believed to evolve in a neutral manner. In order to find the most likely groups on which positive selection has been working, we conducted a series of experiments integrating data from site-based and lineage-specific studies.

Due to their various emphases, we employed many of the selection tests developed in HyPhy v 2.220150316 beta (Pond and Muse 2005) to study the patterns of selection acting on distinct toxin families. The Analyze Codon Data analysis in HyPhy produces overall alignment values, whereas the FUBAR technique assesses the intensity of persistent positive or negative selection on individual amino

acids (Murrell, et al. 2013). The Mixed Effects Model of Evolution (MEME) approach, on the other hand, finds particular locations that have been exposed to positive selection in the past (Murrell, et al. 2012).

Protein Modelling

To map residues evolving under positive selection in three-dimensional (3D) structures, sample sequences from the RCSB PDB database (Rose, et al. 2010) were used to create bespoke models for each clade belonging to various toxin families (Table 1). Alignments of each clade were trimmed to match these PDB structures. To render and colour the 3D structure of the proteins, we utilized the UCSF Chimera program v 1.10.2 with attribute files generated from FUBAR and MEME results. For FUBAR, we used the value from the beta-alpha column which is a measure of the difference between the rates of non-synonymous (beta) and synonymous (alpha) mutations. For MEME, since MEME estimates two rates of positive selection and gives each a probability, we take the weighted average of those two and then subtract alpha to arrive at a similar value to the one we used for FUBAR.

Table 1: Custom models for protein modelling.

Clade	Sequence for 3D modeling	PDB ID
Viperidae	Vipera_ammodytes_ammodytes_P00992	6a5i
DTX	Dendroaspis_polylepis_P00981	1dtk
BTX	Bungaru_ multicinctus_Q1RPT0	1bun
non vipers	Bungarus_multicinctus_Q1RPT0	1bun
Viper type plasmin inhibitor	Vipera_ammodytes_ammodytes_P00992	6a5i
non-viper type plasmin inhibitor	Pseudonaja_textilisQ90WA1	5zj3

Results and Discussion

Diverse kunitz peptides have been characterized as neurotoxins (Harvey and Karlsson 1980; Bohlen, et al. 2011; Baconguis, et al. 2014; Possani, et al. 1992), and our phylogenetic analysis combined with differences in sequence, structure, and function suggest that the evolution of this derived activity has occurred on four independent occasions (Figure 1). The new toxins include monomeric toxins and members of toxin complexes. Dendrotoxins are monomeric toxins from *Dendroaspis* venoms that selectively block $K_V1.1$ voltage-gated potassium channels (Harvey and Karlsson 1980). Kunitz peptides that are subunits of complex neurotoxins may be associated through non-covalent interactions (MitTx and taicatoxin) or covalently linked (β-bungarotoxin). Intriguingly, all such multimers are heteromeric and include PLA_2 toxins. MitTx is a complex of one kunitz subunit and two PLA_2 subunits that activates acid-sensing ion channel ASIC1 to cause intense pain as part of the defensive arsenal of *Micrurus tener*

(Bohlen, et al. 2011; Baconguis, et al. 2014). Taicatoxin was discovered in the venom of *Oxyuranus scutellatus* and is a complex toxin consisting of one 3FTx subunit, one PLA_2 subunit, and 4 kunitz subunits that blocks cardiac voltage-dependent L-type calcium channels (Ca_V) (Possani, et al. 1992). β-bungarotoxins are voltage-gated potassium channels (K_V) blocking heterodimers consisting of a kunitz peptide disulphide-linked to a PLA_2 subunit via a newly evolved cysteine not found in other kunitz peptides, linked to a matching novel cysteine in the PLA_2 subunit that is also not found in other PLA_2 toxins. Our phylogenetic analysis indicates that the characteristic cysteine in β-bungarotoxin kunitz peptides evolved independently on two different occasions (Figure 1). In each case, the cysteine is in the same position, suggesting strong structural selection due to inter-chain structural constraints. However, consistent with the phylogenetic placement into two distinct clades, each type differs in the flanking amino acids. Intriguingly, there appears to have been a secondary loss of this trait occurring in the one of the kunitz peptide clades β-bungarotoxins, with the sequences C5H0E4 (Uniprot ID) and B4ESA2 (Uniprot ID) lacking the diagnostic and structurally necessary cysteine (Figure 1).

Other derived kunitz peptides have the pathophysiological action of inhibiting the clotting regulatory enzyme plasmin, which breaks down blood clots in the body. Unsurprisingly, plasmin inhibitors have been isolated and characterized from venoms which are powerfully procoagulant. The venoms allow the snakes to subjugate their prey by triggering the rampant production of endogenous thrombin, leading to the formation of enough blood clots to induce debilitating and lethal strokes. Such toxins have been well-described for the *Daboia* genus within the Viperidae family, and the *Oxyuranus/Pseudonaja* clade within the Elapidae family (Figures 2 and 3). While *Daboia* venoms produce procoagulant toxicity through the activation of Factor X and *Oxyuranus* and *Pseudonaja* through the activation of prothrombin, both converge on the same functional outcome: the production of high levels of endogenous thrombin which convert fibrinogen to fibrin. Phylogenetic analysis (Figure 1) reveals that they show convergent neofunctionalization of the kunitz peptide such that they inhibit plasmin, thereby prolonging the half-life of the blood clots formed by the venom. Both species also show convergent modification of the same key residue into an arginine, which has been shown to be critical for activity. Both mutants of plasmin inhibitors with only this amino acid changed and native isoforms lacking this arginine from *Pseudonaja* venom were found to not affect plasmin (Flight, et al. 2005; Flight, et al. 2009). Intriguingly, other phylogenetically distinct sequences contain this mutation (Figure 3), the majority of which are in species with procoagulant venoms, including *Oxyuranus* variants that are phylogenetically distinct from the functionally characterized plasmin inhibitors, suggesting that this genus may have evolved plasmin-inhibiting kunitz peptides on multiple occasions. However, functional studies are needed to confirm that these other arginine-containing peptides are indeed plasmin inhibitors.

Selection analyses revealed very different rates of molecular evolution for this toxin type within the snake families (Figure 4 and Table 2), strongly suggesting that there is a multiplicity of undocumented novel activities yet to be discovered across the full range of this toxin class. This is consistent of the documentation of three evolutions of neurotoxin function within just the elapid snakes. The differential rates between the monomeric dendrotoxins (ω=2.10) and the disulphide-linked β-bungarotoxin subunits (ω=1.23) is consistent with the structural constraints imposed upon the β-bungarotoxin subunits by being

not only part of a multi-subunit complex, but a disulphide-linked one at that. However, despite these structural constraints, the β-bungarotoxin subunits display evidence of individual sites under positive selection. In contrast to the neurotoxins, but consistent with the high structural conservation of the enzymatic pathophysiological target, both independent lineages of plasmin inhibitors are under negative purifying selection pressures (Figure 4 and Table 2).

Table 2: Molecular evolutionary rates of kunitz peptides (See Figure 13 for structural models).

Toxin group	ω	FUBAR(-)[a]	FUBAR(+)[b]	MEME[c]	FUBAR & MEME[d]
Viperidae clade	0.96	1	8	8	4
Non-viperid clade	1.18	5	10	13	6
Neurotoxins--Dendrotoxins	2.10	0	6	7	3
Neurotoxins--Bungarotoxins	1.23	15	25	30	22
Plasmin inhibitors *Daboia*	0.80	1	0	2	0
Plasmin inhibitors *Oxyuranus/ Pseudonaja*	0.62	2	0	0	0

[a] Number of codons under negative selection according to FUBAR

[b] Number of codons under positive selection according to FUBAR

[c] Number of codons under episodic diversifying selection according to MEME

[d] Number of codons that fit criteria [b] and [c]

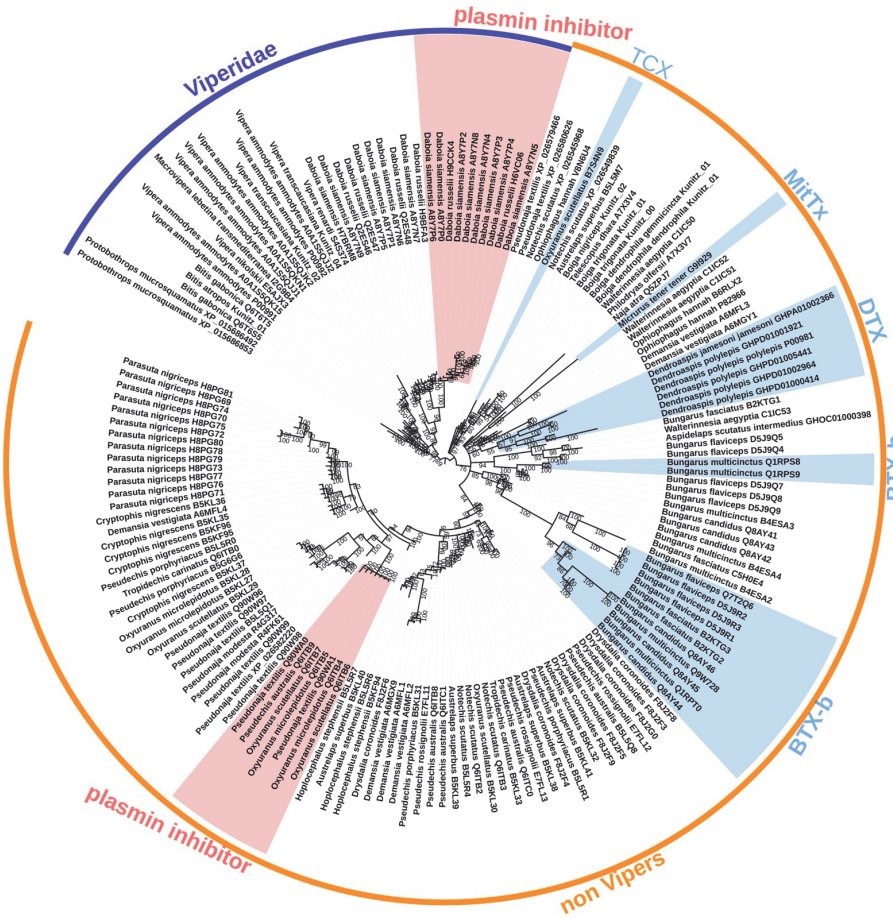

Figure 1: Molecular phylogenetic reconstruction of kunitz peptide toxins. The convergent evolution of coagulotoxins are shaded in red, while the convergent evolution of neurotoxins is highlighted in blue. TCX= taicatoxin. DTX=Dendrotoxin. BTX-b= β-bungarotoxins (characterised by the presence of a novel cysteine). Sequence alignment used for constructing phylogenetic tree can be viewed in Supplementary File 3. For tree output file for kunitz toxins, see Supplementary File 4.

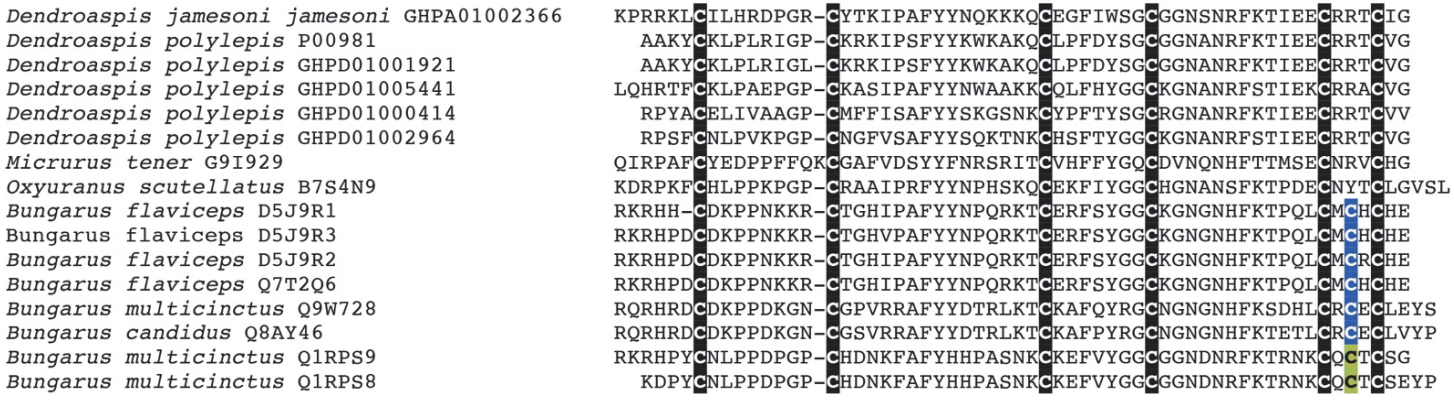

Figure 2: Sequence alignment of representative derived neurotoxic forms of kunitz peptides. Shown are: *Dendroaspis* $K_V1.1$ voltage-gated potassium channel blocking dendrotoxins; *Micrurus* acid-sensing ion channel ASIC1 activating MitTx; *Oxyuranus* cardiac voltage-dependent L-type calcium channels (Ca_V) blocking taicatoxin; and *Bungarus* voltage-gated potassium channels (K_V) blocking bungarotoxins. The convergent evolution of interchain cysteines in the *Bungarus* sequences are indicated by different highlight colours.

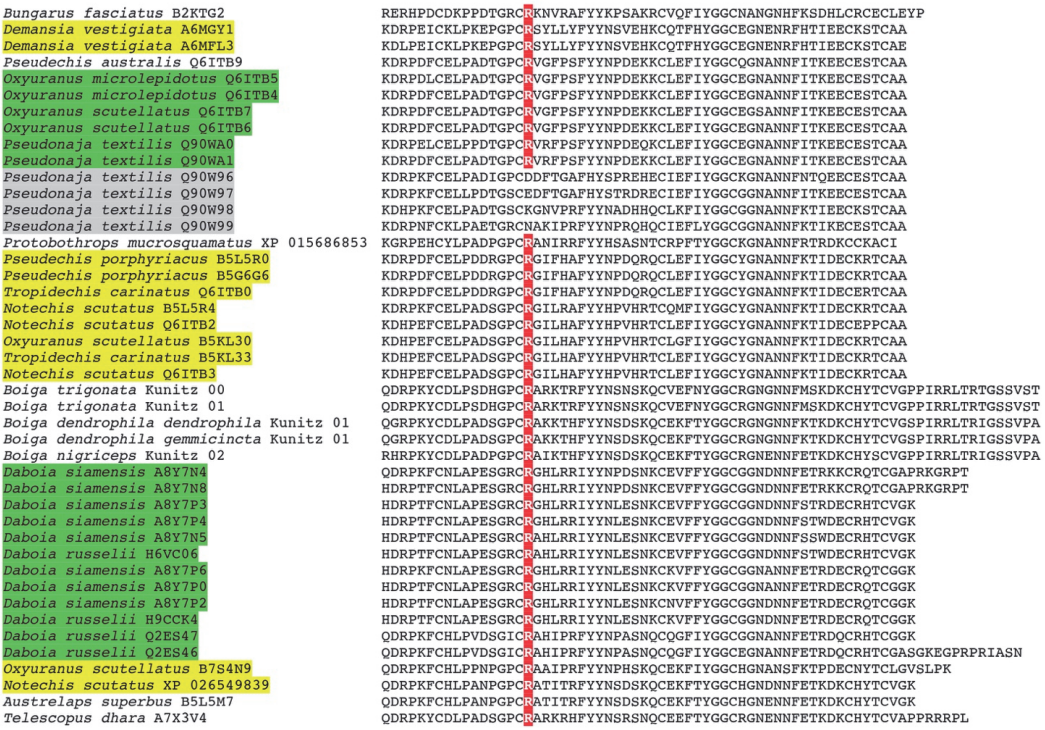

Figure 3: Sequence alignment of representative plasmin-inhibiting derived forms of kunitz peptide toxins, with the functionally important arginine residue shaded in red. Procoagulant species with confirmed plasmin inhibiting activating are shaded in green. Procoagulant species which contain derived kunitz forms with the functionally important arginine but with phylogenetically distinct sequences that have not been functionally confirmed as plasmin-inhibiting are highlighted in yellow. *Pseudonaja* variants which lack the diagnostic arginine and have been bioactivity tested confirm the lack of plasmin inhibition activity are highlighted in gray.

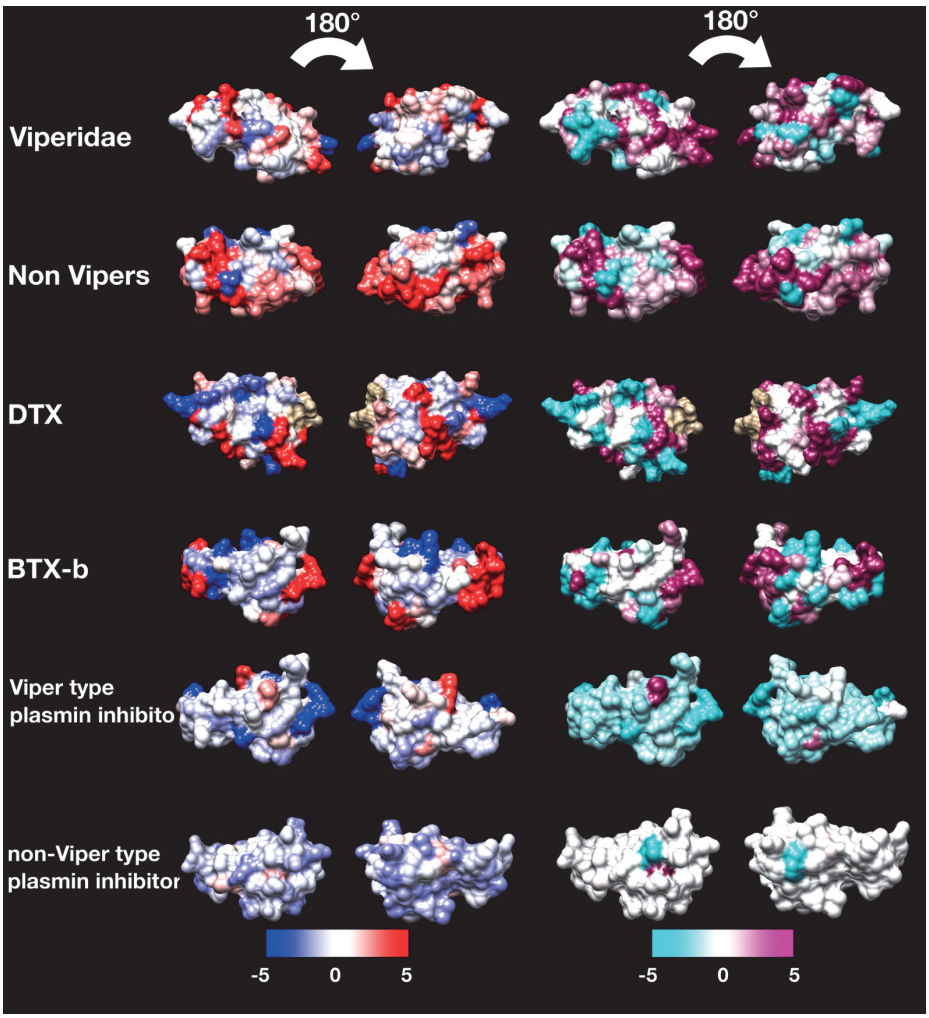

Figure 4: Molecular modelling of kunitz toxins showing sites under selection by FUBAR (left) and MEME (right) colour coded to show sites that are negatively, neutrally, or positively selected. See Table 2 for values. Protein models show front and back views colored according to FUBAR's estimated strength of selection (β-α, left) and MEME's significance levels (right). Table 1 contains the information regarding template choice for each toxin subclass.

References

Antuch W, Berndt KD, Chavez MA, Delfin J, Wuthrich K. 1993. The NMR solution structure of a Kunitz-type proteinase inhibitor from the sea anemone *Stichodactyla helianthus*. European Journal of Biochemistry 212:675-684.

Baconguis I, Bohlen CJ, Goehring A, Julius D, Gouaux E. 2014. X-ray structure of acid-sensing ion channel 1–snake toxin complex reveals open state of a Na^+-selective channel. Cell 156:717-729.

Bayrhuber M, Vijayan V, Ferber M, Graf R, Korukottu J, Imperial J, Garrett JE, Olivera BM, Terlau H, Zweckstetter M. 2005. Conkunitzin-S1 is the first member of a new Kunitz-type neurotoxin family: structural and functional characterization. Journal of Biological Chemistry 280:23766-23770.

Benson DA, Cavanaugh M, Clark K, Karsch-Mizrachi I, Lipman DJ, Ostell J, Sayers EW. 2012. GenBank. Nucleic Acids Research 41:D36-D42.

Beress L. 1982. Biologically active compounds from coelenterates. Pure and Applied Chemistry 54:1981-1994.

Bohlen CJ, Chesler AT, Sharif-Naeini R, Medzihradszky KF, Zhou S, King D, Sánchez EE, Burlingame AL, Basbaum AI, Julius D. 2011. A heteromeric Texas coral snake toxin targets acid-sensing ion channels to produce pain. Nature 479:410-414.

Chang L-s, Chung C, Huang H-B, Lin S-r. 2001. Purification and characterization of a chymotrypsin inhibitor from the venom of *Ophiophagus hannah* (King Cobra). Biochemical and Biophysical Research Communications 283:862-867.

Chen C, Hsu C-H, Su N-Y, Lin Y-C, Chiou S-H, Wu S-H. 2001. Solution structure of a Kunitz-type chymotrypsin inhibitor isolated from the elapid snake *Bungarus fasciatus*. Journal of Biological Chemistry 276:45079-45087.

Edgar RC. 2004. MUSCLE: multiple sequence alignment with high accuracy and high throughput. Nucleic Acids Research 32:1792-1797.

Fiedler F. 1987. Effects of secondary interactions on the kinetics of peptide and peptide ester hydrolysis by tissue kallikrein and trypsin. European Journal of Biochemistry 163:303-312.

Flight S, Johnson L, Trabi M, Gaffney P, Lavin M, de Jersey J, Masci P. 2005. Comparison of textilinin-1 with aprotinin as serine protease inhibitors and as antifibrinolytic agents. Pathophysiology of Haemostasis and Thrombosis 34:188-193.

Flight SM, Johnson LA, Du QS, Warner RL, Trabi M, Gaffney PJ, Lavin MF, De Jersey J, Masci PP. 2009. Textilinin-1, an alternative anti-bleeding agent to aprotinin: importance of plasmin inhibition in controlling blood loss. British Journal of Haematology 145:207-211.

Fry BG, Scheib H, van der Weerd L, Young B, McNaughtan J, Ramjan SR, Vidal N, Poelmann RE, Norman JA. 2008. Evolution of an arsenal: structural and functional diversification of the venom system in the advanced snakes (Caenophidia). Molecular & Cellular Proteomics 7:215-246.

Grzesiak A, Krokoszynska I, Krowarsch D, Buczek O, Dadlez M, Otlewski J. 2000. Inhibition of six serine proteinases of the human coagulation system by mutants of bovine pancreatic trypsin inhibitor. Journal of Biological Chemistry 275:33346-33352.

Guo C-t, McClean S, Shaw C, Rao P-f, Ye M-y, Bjourson AJ. 2013. Trypsin and chymotrypsin inhibitor peptides from the venom of Chinese *Daboia russellii siamensis*. Toxicon 63:154-164.

Harvey A, Karlsson E. 1980. Dendrotoxin from the venom of the green mamba, *Dendroaspis angusticeps*. Naunyn-Schmiedeberg's Archives of Pharmacology 312:1-6.

Harvey A, Robertson B. 2004. Dendrotoxins: structure-activity relationships and effects on potassium ion channels. Current Medicinal Chemistry 11:3065-3072.

Hedstrom L. 2002. Serine protease mechanism and specificity. Chemical reviews 102:4501-4524.

Honma T, Shiomi K. 2006. Peptide toxins in sea anemones: structural and functional aspects. Marine Biotechnology 8:1-10.

Koludarov I, Sunagar K, Undheim EA, Jackson TN, Ruder T, Whitehead D, Saucedo AC, Mora GR, Alagon AC, King G. 2012. Structural and molecular diversification of the Anguimorpha lizard mandibular venom gland system in the arboreal species *Abronia graminea*. Journal of Molecular Evolution 75:168-183.

Larsson A. 2014. AliView: a fast and lightweight alignment viewer and editor for large datasets. Bioinformatics 30:3276-3278.

Laskowski Jr M, Kato I. 1980. Protein inhibitors of proteinases. Annual Review of Biochemistry 49:593-626.

Letunic I, Bork P. 2007. Interactive Tree Of Life (iTOL): an online tool for phylogenetic tree display and annotation. Bioinformatics 23:127-128.

Minagawa S, Ishida M, Shimakura K, Nagashima Y, Shiomi K. 1997. Isolation and amino acid sequences of two Kunitz-type protease inhibitors from the sea anemone *Anthopleura aff. xanthogrammica*. Comparative Biochemistry and Physiology Part B: Biochemistry and Molecular Biology 118:381-386.

Murrell B, Moola S, Mabona A, Weighill T, Sheward D, Kosakovsky Pond SL, Scheffler K. 2013. FUBAR: a fast, unconstrained bayesian approximation for inferring selection. Molecular Biology and Evolution 30:1196-1205.

Murrell B, Wertheim JO, Moola S, Weighill T, Scheffler K, Pond SLK. 2012. Detecting individual sites subject to episodic diversifying selection. PLoS Genetic 8:e1002764.

Navaneetham D, Sinha D, Walsh PN. 2010. Mechanisms and specificity of factor XIa and trypsin inhibition by protease nexin 2 and basic pancreatic trypsin inhibitor. The Journal of Biochemistry 148:467-479.

Pond SL, Muse SV. 2005. HyPhy: hypothesis testing using phylogenies. In: Statistical Methods in Molecular Evolution: Springer. p. 125-181.

Possani LD, Martin BM, Yatani A, Mochca-Morales J, Zamudio FZ, Gurrola GB, Brown AM. 1992. Isolation and physiological characterization of taicatoxin, a complex toxin with specific effects on calcium channels. Toxicon 30:1343-1364.

Ronquist F, Teslenko M, Van Der Mark P, Ayres DL, Darling A, Höhna S, Larget B, Liu L, Suchard MA, Huelsenbeck JP. 2012. MrBayes 3.2: efficient Bayesian phylogenetic inference and model choice across a large model space. Systematic Biology 61:539-542.

Rose PW, Beran B, Bi C, Bluhm WF, Dimitropoulos D, Goodsell DS, Prlić A, Quesada M, Quinn GB, Westbrook JD. 2010. The RCSB Protein Data Bank: redesigned web site and web services. Nucleic Acids Research 39:D392-D401.

Scheidig AJ, Hynes TR, Pelletier LA, Wells JA, Kossiakoff AA. 1997. Crystal structures of bovine chymotrypsin and trypsin complexed to the inhibitor domain of alzheimer's amyloid β-protein precursor (APPI) and basic pancreatic trypsin inhibitor (BPTI): Engineering of inhibitors with altered specificities. Protein Science 6:1806-1824.

Van Nostrand WE, Schmaier AH, Siegel RS, Wagner SL, Raschke WC. 1995. Enhanced plasmin inhibition by a reactive center lysine mutant of the Kunitz-type protease inhibitor domain of the amyloid β-protein precursor. Journal of Biological Chemistry 270:22827-22830.

Wan H, Lee KS, Kim BY, Zou FM, Yoon HJ, Je YH, Li J, Jin BR. 2013. A spider-derived Kunitz-type serine protease inhibitor that acts as a plasmin inhibitor and an elastase inhibitor. PLoS One 8:e53343.

Wang H, Wang L, Zhou M, Yang M, Ma C, Chen T, Zhang Y, Zeller M, Hornshaw M, Shaw C. 2012. Functional peptidomics of amphibian skin secretion: a novel Kunitz-type chymotrypsin inhibitor from the African hyperoliid frog, *Kassina senegalensis*. Biochimie 94:891-899.

Wells JM, Strickland S. 1994. Aprotinin, a Kunitz-type protease inhibitor, stimulates skeletal muscle differentiation. Development 120:3639-3647.